Selcuk Journal of Agriculture and Food Sciences
https://dergipark.org.tr/tr/pub/selcukjafsci
Research Article

(2026) 40 (2), 361-376 DOI:10.15316/selcukjafsci.1821374 e-ISSN: 2458-8377 Selcuk J Agr Food Sci

Projected Variations in Reference Crop Evapotranspiration Across Türkiye

Ali Kaan Yetik*, Burak Nazmi Candoğan[2]

[1] Niğde Ömer Halisdemir University, Agricultural Sciences and Technologies, Department of Biosystems Engineering, Niğde, Türkiye

[2] Bursa Uludağ University, Faculty of Agriculture, Department of Biosystems Engineering, Bursa, Türkiye

HIGHLIGHTS

- Projections show significant ETo increases across Türkiye.
- The far-future RCP8.5 scenario yields the highest ETo rise.
- Rising ETo values suggest escalating agricultural water needs.

Abstract

Climate change is expected to intensify evapotranspiration dynamics globally, posing significant challenges for sustainable water management and agricultural productivity. This study assessed the spatial and temporal variability of reference crop evapotranspiration (ETo) across Türkiye using the HADGEM climate model under RCP4.5 and RCP8.5 scenarios for the near (2023-2052) and far future (2069-2098) periods, relative to the reference baseline (1971-2000). ETo was estimated using the FAO Penman Monteith equation by ETo Calculator, while temporal persistence and variability were examined through the Spearman rank correlation and coefficient of variation, respectively. Results revealed a widespread and statistically significant increase in ETo across most regions, with the most pronounced changes occurring under the far-future RCP8.5 scenario. Average ETo increases exceeded 25% in continental and southern provinces such as Isparta, Niğde, and Gaziantep, while the humid Black Sea region remained the least affected, showing increases below 20%. Seasonal analyses identified summer as the most stable yet intense evaporative period, and winter as the season with the highest variability. These findings indicate that rising temperatures and altered humidity-radiation interactions will substantially increase evaporative demand and irrigation requirements. Consequently, region-specific adaptation strategies and integrated water management policies will be critical to ensure agricultural resilience under future climate conditions.

Keywords: Climate Change, HADGEM, Penman-Monteith, Spatial Variability, Spearman Correlation

1. Introduction

Climate change has emerged as one of the most critical global environmental challenges, leading to significant alterations in atmospheric, oceanic, and terrestrial systems (Reid et al. 2009). Variations in precipitation, wind speed, humidity, temperature, vapor pressure, and solar radiation are increasingly

Citation: Yetik, A. K., & Candoğan, B. N. (2026). Projected Variations in Reference Crop Evapotranspiration Across Türkiye. *Selcuk Journal of Agriculture and Food Sciences*, 40 (2), 361-376. https://doi.org/10.15316/selcukjafsci.1821374
Corresponding Author E-mail: alikaanyetik@ohu.edu.tr

Received date: 11/11/2025
Accepted date: 15/06/2026

attributed to climate change (Leng et al. 2015; Danandeh Mehr et al. 2020). Specifically, these changes have intensified since the Industrial Revolution, are closely linked to anthropogenic activities such as fossil fuel combustion, deforestation, and industrial expansion, which have substantially increased greenhouse gas emissions and disrupted atmospheric balance. As a consequence, global mean temperature has risen, sea levels have increased, and the frequency and intensity of extreme weather events have become more pronounced (Easterling et al. 2000; Meehl et al. 2000). Numerous studies have shown that climate change poses serious risks to human health, agricultural production, water resources, ecosystems, and economies worldwide (Myers and Patz 2009; McMichael and Lindgren 2011; Ayas 2019; Gomez-Zavaglia et al. 2020). Türkiye is located within the Mediterranean climate transition zone and is considered highly sensitive to climate change because of its pronounced regional contrasts in temperature, precipitation, aridity, and topography (Yetik et al. 2024). National-scale projections have indicated rising temperatures, seasonal shifts in precipitation, and increasing pressure on water resources, especially in semi-arid and continental regions. These changes are expected to directly influence the atmospheric drivers of evapotranspiration and, consequently, irrigation demand, crop water use, and basin-scale water allocation in different agro-climatic regions of the country.

Water is indispensable for sustaining life, and its efficient use is crucial for both human survival and agricultural productivity. The formulation of sound water-use policies, particularly those targeting groundwater sustainability, is essential for mitigating the growing impacts of climate change (Calzadilla et al. 2010). In many developing and underdeveloped countries, current water management strategies are insufficient to cope with the threats posed by changing climate and drought. Therefore, adaptation-oriented studies that aim to mitigate these effects and improve resilience have gained importance. In this context, modern irrigation techniques, water-harvesting systems, and deficit irrigation strategies have been proposed to optimize water use in agriculture. Among these strategies, estimating crop water consumption remains one of the most effective methods to enhance agricultural sustainability and water productivity.

The concept of reference crop evapotranspiration (ETo) is central to understanding plant-water-atmosphere interactions under varying climatic conditions. Allen et al. (1998) noted that although empirical equations for estimating evapotranspiration may perform adequately under specific local conditions, their applicability diminishes under different climatic settings. Consequently, researchers have developed standardized ETo estimation methods that provide a reference value applicable to different crops and regions (Droogers and Allen 2002). ETo plays a vital role in hydrological modelling, irrigation management, and sustainable agricultural practices, serving as a key component of the hydrological cycle in agroecosystems (Fan et al. 2016). Over the decades, several ETo estimation methods have been proposed, ranging from temperature-based equations (Thornthwaite, Hargreaves-Samani, Blaney Criddle) to radiation and combination methods (Jensen-Haise, Penman Monteith). Among these, the FAO-56 Penman Monteith method has become the global standard due to its robust physical basis and reliable performance across different climatic zones (Allen et al. 1998; Walter et al. 2000; Karaer et al. 2023). This method integrates key meteorological parameters (air temperature, relative humidity, wind speed, and solar radiation) allowing accurate and consistent ETo estimation. Because these parameters are directly influenced by climate change, ETo values are expected to undergo significant alterations in future periods (Thomas 2000; Deveci and Konukçu 2024).

Numerous studies have investigated temporal and spatial changes in ETo under past and projected climate conditions. For instance, Jun et al. (2012) examined meteorological variations over the Yunnan region of China between 1961 and 2010 and found insignificant trends in ETo despite declining solar radiation. He et al. (2013) reported a 1.5°C temperature rise between 1961 and 2009, leading to a significant increase in ETo. Mojid et al. (2015) observed decreasing ETo trends in Bangladesh due to reduced net radiation and wind speed. Using the CNRM-CM5 regional model, Liu et al. (2021) projected a marked increase in ETo over the Poyang Lake Basin by 2100 under RCP4.5 and RCP8.5 scenarios, particularly during 2041-2070. Similarly, Di Nunno and Granata (2023) employed the MLP-M5P model in Sicily (Italy) and identified considerable ETo increases in future projections. Studies conducted in India (Kingra et al. 2024), North America (Shamir et al. 2024), and South Africa (Woyessa 2024) also confirmed region-specific ETo increases linked to rising temperatures and radiation levels.

At the national scale, limited research has focused on assessing future ETo trends. Nistor et al. (2019) analyzed evapotranspiration projections for 2011-2070 using CMIP5 multi-model ensembles and reported substantial ETo increases, particularly in the Mediterranean and southeastern regions. Ünlükara et al. (2011) calculated monthly ETo values in Konya and Karaman using the FAO-56 Penman Monteith method and found varying seasonal trends, while Bora et al. (2015) identified increasing ETo during summer and decreasing values in winter for the Menemen Plain. Arslan (2017) used Turc and Coutagne formulas for Niğde and reported a non-significant but positive trend. In Marmara, Arabi and Candoğan (2022) found spatial variations in ETo, with increasing trends in western areas and declining values in northern stations. Kum (2022) highlighted distinct ETo increases in southern Şanlıurfa, emphasizing the importance of evapotranspiration for local irrigation management.

However, most of these studies were conducted at local or regional scales and often relied on different estimation methods or limited climate models. A comprehensive, country-wide assessment of ETo dynamics based on the future estimations of HADGEM model under RCP4.5 and RCP8.5 scenarios has not yet been conducted for Türkiye. This study aims to evaluate the projected spatial and temporal variations of reference crop evapotranspiration (ETo) across Türkiye under the RCP4.5 and RCP8.5 climate scenarios. Specifically, the study (i) quantifies seasonal and annual changes in ETo relative to the reference period, (ii) compares near-future and far-future responses across provinces, and (iii) maps the spatial distribution of projected ETo variability to support national-scale agricultural water management and climate adaptation planning.

2. Materials and Methods

2.1. Study area

The study was conducted across all 81 provinces of Türkiye, representing diverse climatic regions ranging from humid coastal zones to semi-arid continental interiors. The geographical coordinates and elevations of these stations are presented in Table 1.

Table 1. Locations and altitudes of meteorological stations used in the study across Türkiye

Station	Latitude (°N)	Longitude (°E)	Altitude (m)	Station	Latitude (°N)	Longitude (°E)	Altitude (m)
Adana	37.09	35.32	23	K. maraş	37.54	36.99	568
Adıyaman	37.82	38.19	669	Karabük	41.26	32.72	354
Afyon	38.70	30.47	1034	Karaman	37.17	33.24	1039
Ağrı	39.74	43.07	1632	Kars	40.68	43.03	1768
Aksaray	38.44	34.01	978	Kastamonu	41.42	33.72	775
Amasya	40.58	35.87	411	Kayseri	38.74	35.46	1054
Ankara	39.96	32.90	938	Kırıkkale	39.75	33.62	712
Antalya	36.85	30.92	54	Kırklareli	41.82	27.26	203
Ardahan	41.11	42.62	1900	Kırşehir	39.18	34.06	991
Artvin	41.19	41.89	345	Kilis	36.79	37.14	660
Aydın	37.76	27.90	67	Kocaeli	40.74	30.00	4
Balıkesir	40.35	28.05	70	Konya	37.93	32.58	1031
Bartın	41.65	32.24	25	Kütahya	39.44	30.00	970
Batman	37.89	41.27	550	Malatya	38.37	38.26	954
Bayburt	40.24	40.23	1550	Manisa	38.67	27.39	71
Bilecik	40.19	30.00	500	Mardin	37.40	40.71	1083
Bingöl	38.91	40.49	1151	Mersin	36.94	34.61	10
Bitlis	38.54	42.10	1637	Muğla	37.21	28.38	660
Bolu	40.73	31.71	725	Muş	38.81	41.43	1350
Burdur	37.78	30.23	950	Nevşehir	38.59	34.73	1224
Bursa	40.18	29.03	100	Niğde	38.04	34.69	1229
Çanakkale	40.31	26.35	2	Ordu	40.82	37.86	5
Çankırı	40.68	33.67	800	Osmaniye	37.03	36.24	129
Çorum	40.63	34.89	801	Rize	40.96	40.60	6
Denizli	37.78	29.07	324	Sakarya	40.74	30.49	31
Diyarbakır	37.81	40.31	686	Samsun	41.31	36.19	4

Düzce	40.92	31.23	150	Siirt	38.00	41.99	986
Edirne	41.61	26.52	42	Sinop	41.93	35.00	0
Elâzığ	38.66	39.26	1067	Sivas	39.76	37.00	1285
Erzincan	39.76	39.42	1185	Şanlıurfa	37.21	38.81	477
Erzurum	39.96	41.16	1890	Şırnak	37.42	42.12	377
Eskişehir	39.81	30.48	788	Tekirdağ	41.08	27.54	37
Gaziantep	37.14	37.41	850	Tokat	40.35	36.58	623
Giresun	40.78	38.35	14	Trabzon	40.84	39.84	0
Gümüşhane	40.50	39.54	1153	Tunceli	39.19	39.58	922
Hakkâri	37.58	43.80	1720	Uşak	38.70	29.29	890
Hatay	36.12	36.15	67	Van	38.40	43.27	1726
Iğdır	39.98	44.10	850	Yalova	40.55	29.27	30
Isparta	37.78	30.47	1049	Yozgat	39.89	34.83	1300
İstanbul	41.11	28.77	40	Zonguldak	41.28	31.73	60
İzmir	38.48	27.17	2				

2.2. Climate Data

The climate scenario data used in this study were not generated de novo within the manuscript. Instead, the study adopted the official Türkiye climate projection framework produced by the Turkish State Meteorological Service within TR2015-CC, in which HadGEM2-ES outputs were dynamically downscaled with the RegCM4.3.4 regional climate model to 20 km resolution over a domain covering Türkiye and its surroundings (Akçakaya et al. 2015; Demircan et al. 2017). The published configuration of that framework includes one-way nesting, a 130 × 180 grid, and 18 sigma levels, together with the BATS land-surface scheme, Holtslag boundary-layer scheme, CCM3 radiation scheme, Zeng et al. surface-flux formulation, Hsie et al. explicit moisture scheme, Pal et al. large-scale cloud/precipitation treatment, and Emanuel-over-land / Grell-over-sea cumulus parameterization (Demircan et al. 2017). In the present manuscript, RF (1971-2000) represents the reference simulation of this adopted model framework rather than an observation-based climatology. The future windows analyzed in this study (2023-2052 and 2069-2098) were extracted from the same scenario chain under RCP4.5 and RCP8.5, thereby preserving internal consistency among the reference and future ETo estimates.

Because the present manuscript does not rerun the regional climate model, it does not present a new province-by-province historical validation of all daily meteorological drivers with RMSE, MAE, and R2. Instead, it uses an adopted projection dataset whose underlying framework was previously subjected to control/sensitivity evaluation for key climate fields such as temperature and precipitation in the reference period against gridded observation datasets (Demircan et al. 2017). Therefore, the results are interpreted here as scenario-based provincial-scale ETo estimates within a consistent projection framework rather than as deterministic local forecasts.

Table 2. Description of the scenarios

Scenario	Model	Period	RCP Value
RF-45	HADGEM	1971-2000 (Reference, RF)	-
N-45		2023-2052 (Near Future, N)	4.5
N-85			8.5
F-45		2069-2098 (Far Future, F)	4.5
F-85			8.5

2.3. Calculation of Reference Crop Evapotranspiration

Daily ETo values for each station were calculated using the FAO Penman Monteith equation, which is the universally accepted standard for estimating reference crop evapotranspiration (Allen et al. 1998). The required input parameters for this method include daily maximum and minimum air temperature (°C), sunshine duration (hours), relative humidity (%), and wind speed (m s^{-1}). All calculations were performed using the FAO ETo Calculator software (Raes and Muñoz 2009) by Equation 1.

$$ETo = \frac{0.408\Delta(R_n - G) + \gamma\left(\frac{900}{T+273}\right)u_2(e_s - e_a)}{\Delta + \gamma(1 + 0.34u_2)} \quad (1)$$

Where ETo is the reference crop evapotranspiration (mm day^{-1}), R_n is the net radiation at the crop surface (MJ m^{-2} day^{-1}), G is the soil heat flux density (MJ m^{-2} day^{-1}), T is the mean daily air temperature (°C), u_2 is the wind speed at 2 m height (m s^{-1}), e_s is the saturation vapor pressure (kPa), e_a is the actual vapor pressure (kPa), (e_s - e_a) is the saturation vapor pressure deficit (kPa), Δ is the slope of the vapor pressure curve (kPa $°C^{-1}$), and γ is the psychrometric constant (kPa $°C^{-1}$). Wind speed was standardized to the 2 m height required by FAO-56 using the logarithmic wind profile relation $u_2 = u_z \times 4.87 / \ln(67.8z - 5.42)$, where u_z is wind speed at measurement height z (10 m) and u_2 is the equivalent wind speed at 2 m (Allen et al. 1998). Radiation-related terms were derived within the FAO-56 Penman-Monteith workflow from sunshine-duration based inputs and the associated astronomical relations implemented in the FAO ETo Calculator. Daily ETo values were then aggregated to monthly, seasonal, and annual values for each province.

Monthly, seasonal and annual ETo values were computed for each province. Seasonal means were calculated as follows: December-February (winter), March-May (spring), June-August (summer), and September-November (autumn).

2.4. Spearman rank correlation and coefficient of variation analyses of ETo series

To examine the temporal behavior and internal variability of the ETo series, a combination of correlation and dispersion analyses was conducted. First, the monotonic temporal relationships within ETo data of each province were assessed using the non-parametric Spearman rank correlation coefficient (r_s), a distribution-free alternative to Pearson's correlation (Zar 2005). The coefficient was computed as shown in Equation 2.

$$r_s = 1 - \frac{6\sum {d_i}^2}{n(n^2 - 1)} \quad (2)$$

where d_i represents the difference between the ranks of paired observations, and n is the number of observations. Values of r_s approaching +1 or −1 indicate strong positive or negative monotonic trends, respectively. The statistical significance of these trends was evaluated at the 5% level ($p < 0.05$). To quantify the dispersion of ETo values over time, the coefficient of variation (CV) was calculated according to Equation 3 (Landsea and Gray 1992).

$$CV = \frac{\sigma_x}{\bar{x}} \quad (3)$$

where σ_x is the standard deviation and $\bar{x}$ is the average of the ETo values. The spatial distribution of r_s and CV was then mapped to identify regions exhibiting consistent monotonic tendencies and inter-annual variability patterns. Spearman rank correlation was retained to represent the direction and significance of monotonic temporal behavior across the provincial ETo series. Trend-magnitude approaches such as Mann-Kendall and Sen's slope can provide additional detail and are recommended for future expanded analyses. Because presenting full province-by-province outputs for these complementary tests would substantially enlarge the manuscript, the current paper retains a compact trend presentation focused on r_s and CV

2.5. Spatial Visualization

To illustrate the spatial and temporal dynamics of ETo across Türkiye, the calculated seasonal and annual values were visualized using ArcGIS 10.2. The Inverse Distance Weighting (IDW) interpolation method was applied to generate continuous spatial distribution maps of ETo and its temporal trends (Singh and Chowdhury 1986; Lebel et al. 1987). IDW was preferred due to its computational simplicity, smooth surface generation, and suitability for uniformly distributed station data (Lu and Wong 2008). The interpolation was performed using a power parameter of 2 and a 12-point neighborhood, which provided a balance between local sensitivity and surface smoothness. To ensure reliability, several test interpolations were compared with alternative power values, and the resulting maps showed consistent spatial patterns without edge artifacts. Therefore, the IDW method was deemed appropriate for representing the spatial variability of ETo. In this study, IDW was used as a descriptive visualization tool to display generalized provincial-scale spatial patterns of ETo rather than to produce terrain-corrected local predictions. Topography-aware geostatistical approaches such as co-kriging or regression kriging may improve local representation in areas with strong elevation gradients and should be considered in future high-resolution regional studies.

3. Results and Discussion

3.1. Projected Changes in Annual Mean ETo

Projected changes in annual mean ETo were evaluated for the near-future (2023-2052, N-45 and N-85) and far-future (2069-2098, F-45 and F-85) periods using the HADGEM model under RCP4.5 and RCP8.5 scenarios. Table 3 summarizes the percentage change in ETo relative to the reference period (1971-2000, RF) for all provinces.

Table 3. Annual mean ETo values (mm day^{-1}) and relative changes (%) across 81 provinces of Türkiye for RCP4.5 and RCP8.5 scenarios compared with the reference period (1971-2000).

	N-45		N-85		F-45		F-85			N-45		N-85		F-45		F-85	
Station	ETo	Δ%	ETo	Δ%	ETo	Δ%	ETo	Δ%	Station	ETo	Δ%	ETo	Δ%	ETo	Δ%	ETo	Δ%
Adana	3.8	7.6*	3.8	9.3	3.9	12.1	4.2	19.6	K. maraş	3.7	11.8	3.8	13.2	3.9	18.0	4.3	28.3
Adıyaman	3.9	11.0	3.9	12.2	4.1	17.7	4.4	26.3	Karabük	3.2	9.9	3.2	10.2	3.2	11.2	3.5	21.2
Afyon	3.5	11.2	3.6	12.7	3.7	16.2	4.0	27.5	Karaman	3.5	9.6	3.6	10.5	3.7	14.1	4.0	23.3
Ağrı	2.9	10.3	2.9	11.0	3.0	15.1	3.3	26.3	Kars	2.7	9.2	2.7	10.8	2.8	14.2	3.1	25.1
Aksaray	3.7	10.8	3.8	11.6	3.9	15.1	4.3	26.2	Kastamonu	3.1	11.0	3.2	11.9	3.2	13.1	3.5	24.1
Amasya	3.3	10.3	3.3	10.7	3.4	13.5	3.7	22.9	Kayseri	3.3	10.6	3.3	12.5	3.4	15.5	3.7	26.2
Ankara	3.3	10.4	3.4	11.4	3.4	13.7	3.8	25.2	Kilis	4.2	10.6	4.2	11.9	4.4	16.6	4.8	26.6
Antakya	3.6	9.0	3.7	10.5	3.8	13.9	4.1	22.6	Kırıkkale	3.4	10.1	3.5	10.8	3.6	13.6	3.9	24.4
Antalya	4.1	7.7	4.1	8.8	4.2	11.9	4.5	18.8	Kırklareli	3.7	11.7	3.7	12.5	3.8	14.6	4.2	27.1
Ardahan	2.6	9.6	2.7	11.4	2.7	14.4	3.0	27.0	Kırşehir	3.5	10.4	3.5	11.2	3.6	14.1	4.0	24.7
Artvin	2.5	9.6	2.6	11.7	2.7	14.2	2.9	26.2	Kocaeli	3.5	9.8	3.5	10.8	3.5	12.8	3.8	22.0
Aydın	3.9	8.5	3.9	9.3	4.1	13.5	4.5	23.9	Konya	3.5	9.1	3.5	10.0	3.7	13.5	4.0	23.1
Balıkesir	3.7	10.8	3.7	11.4	3.8	14.6	4.2	25.4	Kütahya	3.4	11.5	3.5	13.1	3.5	15.9	3.9	28.3
Bartın	3.5	9.0	3.5	9.2	3.5	9.8	3.8	19.3	Malatya	3.4	10.3	3.5	11.2	3.6	15.7	3.9	24.7
Batman	3.7	8.2	3.7	9.4	3.8	12.3	4.1	19.8	Manisa	4.3	10.9	4.3	10.2	4.4	14.9	4.9	27.4
Bayburt	2.7	10.5	2.8	12.0	2.8	15.3	3.1	27.9	Mardin	4.0	8.6	4.1	10.8	4.2	13.8	4.5	21.0
Bilecik	3.4	10.1	3.4	11.1	3.5	13.2	3.8	23.5	Mersin	3.9	7.7	3.9	9.1	4.0	12.1	4.3	19.2
Bingöl	3.1	10.6	3.2	11.9	3.3	15.4	3.5	24.0	Muğla	3.6	7.2	3.7	9.5	3.8	11.8	4.1	21.2
Bitlis	3.2	10.1	3.2	11.0	3.3	14.6	3.6	24.9	Muş	3.0	9.8	3.0	10.5	3.1	14.2	3.3	23.0
Bolu	3.1	11.0	3.1	12.2	3.2	13.4	3.5	25.1	Nevşehir	3.4	10.1	3.4	11.2	3.5	14.3	3.8	23.9
Burdur	3.6	10.6	3.7	12.7	3.8	16.6	4.2	28.9	Niğde	3.3	11.5	3.4	13.3	3.5	16.7	3.8	28.7
Bursa	3.8	11.4	3.8	11.6	3.9	14.5	4.3	25.3	Ordu	2.9	8.1	2.9	8.4	3.0	10.8	3.2	18.1
Çanakkale	4.1	11.5	4.1	11.0	4.2	14.2	4.7	27.2	Osmaniye	3.5	8.2	3.6	10.1	3.6	12.4	3.9	20.0
Çankırı	3.2	11.0	3.2	11.5	3.3	14.0	3.6	25.7	Rize	3.5	8.8	3.5	9.9	3.6	11.0	3.8	18.9
Çorum	3.4	10.6	3.4	11.2	3.5	13.7	3.8	24.5	Sakarya	3.4	9.3	3.4	10.1	3.5	12.1	3.7	20.8
Denizli	3.8	9.8	3.9	11.2	4.0	14.6	4.4	25.4	Samsun	3.4	9.8	3.4	9.1	3.5	12.3	3.7	20.8
Diyarbakır	3.9	8.4	3.9	9.8	4.1	12.9	4.3	20.4	Şanlıurfa	4.4	9.4	4.4	10.6	4.6	14.7	4.9	22.2
Düzce	3.2	9.5	3.2	9.8	3.3	11.4	3.6	20.1	Siirt	3.5	9.2	3.5	10.2	3.6	13.1	3.8	21.0
Edirne	3.8	10.8	3.9	11.3	3.9	13.0	4.3	25.2	Sinop	3.4	8.7	3.3	8.3	3.4	10.4	3.7	19.5
Elâzığ	3.2	9.2	3.2	10.4	3.4	14.2	3.6	22.4	Şırnak	3.8	8.8	3.8	10.0	3.9	12.7	4.2	19.9
Erzincan	2.8	11.6	2.8	13.0	2.9	16.5	3.2	29.5	Sivas	3.0	10.8	3.0	12.3	3.1	15.0	3.4	26.0
Erzurum	2.7	10.5	2.8	12.0	2.8	15.8	3.1	28.0	Tekirdağ	4.0	9.7	4.0	10.4	4.1	12.4	4.5	23.9
Eskişehir	3.4	9.9	3.5	11.5	3.5	13.3	3.9	24.2	Tokat	3.1	10.8	3.1	11.9	3.2	14.2	3.5	24.7
Gaziantep	4.1	11.5	4.1	12.8	4.3	18.1	4.7	28.7	Trabzon	2.6	7.2	2.7	8.2	2.7	10.4	2.9	17.2
Giresun	2.8	8.1	2.8	9.0	2.9	11.2	3.1	19.1	Tunceli	3.0	11.4	3.1	12.8	3.2	17.0	3.5	27.1
Gümüşhane	2.7	11.1	2.8	13.0	2.8	15.4	3.1	27.6	Uşak	3.9	11.1	3.9	11.8	4.1	15.8	4.5	28.1
Hakkâri	3.0	8.7	3.1	12.0	3.1	13.4	3.5	26.7	Van	3.1	10.2	3.2	11.5	3.3	15.1	3.6	26.5

Iğdır	3.0	6.7	3.1	8.0	3.2	10.8	3.4	19.1	Yalova	3.6	10.2	3.6	10.4	3.7	13.2	4.0	23.4
Isparta	3.5	10.8	3.5	12.5	3.7	17.0	4.1	29.3	Yozgat	3.3	10.9	3.4	11.9	3.4	14.4	3.8	25.7
İstanbul	3.7	9.6	3.8	10.2	3.8	12.7	4.2	22.9	Zonguldak	3.3	8.6	3.3	8.7	3.3	9.8	3.6	18.5
İzmir	4.3	11.4	4.2	10.6	4.4	15.3	4.9	27.6									

*Change rate was calculated as [(Period value - Reference value) / Reference value] × 100; N-45, N-85, F-45, and F-85 denote near-future (2023-2052) and far-future (2069-2098) periods under the RCP4.5 and RCP8.5 scenarios, respectively.

As shown in Table 3, the highest mean increases in ETo were projected under the F-85 scenario of the HADGEM model. At the provincial scale, the greatest increases are expected in Erzincan and Isparta, where ETo is projected to rise by 29.48% and 29.30%, respectively, during the F-85 period. In contrast, the lowest increases are projected for Trabzon (17.23%) and Ordu (18.05%), both located in the humid Black Sea region. The smallest overall changes in ETo were observed for the N-45 scenario, reflecting the moderate radiative forcing and temperature increase associated with this pathway. Among all provinces, Erzincan exhibited the highest projected increase, reaching 29.48% under the F-85 scenario, indicating a strong sensitivity of ETo to elevated temperature and radiation conditions in continental regions. Consistent with these findings, Nistor et al. (2019) reported that annual ETo across Türkiye may increase by approximately 21% during the 21st century. They further emphasized that this rise in ETo would directly affect crop water consumption, thereby increasing irrigation requirements and exerting additional pressure on agricultural water management. Several climatic factors influence ETo, including both water-related variables such as relative humidity and energy-related components such as solar radiation, air temperature, vapor pressure, and wind speed. These parameters are interdependent and may influence each other through complex feedback mechanisms (Li et al. 2016).

3.2. Spatial and Temporal Variability of ETo

The spatial and temporal variability of ETo was evaluated using the Spearman rank correlation and CV based on HADGEM outputs. Interpreting these two metrics together provides insight into both the direction and magnitude of temporal behavior. Strong correlations accompanied by low CV values indicate consistent and persistent monotonic trends, whereas high CV values suggest greater fluctuations within the series, even under weak directional tendencies (Helsel and Hirsch 1993; Montgomery and Runger 2010).

During the reference period (1971-2000), spatial patterns revealed regionally distinct relationships across Türkiye (Figure 1). In winter (Figure 1A), negative correlations were concentrated over the Marmara region, indicating stable but slightly declining evaporative demand. No statistically significant increasing trends were detected nationwide, consistent with the weak evaporative dynamics typical of the cold season (Zeng et al. 2021). In spring (Figure 1B), positive correlations dominated most of the country, with the strongest signals over the Black Sea coast (particularly in Trabzon, Giresun, and Artvin) where significant correlations ($p < 0.05$) coincided with moderate CV values. Southeastern provinces such as Diyarbakır, Mardin, and Van exhibited weak negative trends. Ünlükara et al. (2011) similarly found no significant spring trends for Konya and Karaman, supporting the regional stability observed here. The summer season (Figure 1C) showed the highest mean ETo levels yet low interannual variability, as reflected by small CV values. Correlation patterns were generally positive across western and northern Türkiye, while slight negative r_s values appeared locally in the southeast. This suggests a sustained increase in ETo magnitude rather than a shift in temporal direction (Guo et al. 2017). In autumn (Figure 1D), positive correlations prevailed throughout the country, while localized declines occurred in eastern Anatolia and the northeastern Black Sea. CV values ranged mostly between 6-8%, denoting moderate intra-seasonal variability. Statistically significant positive correlations were observed in Çorum, Diyarbakır, and Adıyaman, indicating intensifying evaporative activity. On an annual scale (Figure 1E), positive correlations dominated across Türkiye, with weak negative values limited to parts of eastern and southeastern regions. Significant positive relationships in Mersin, Çorum, Amasya, and Giresun highlight areas of increasing evaporative potential. These findings align with previous regional observations by Altındağ (2007) and Nistor et al. (2019), both reporting a consistent upward tendency in reference crop evapotranspiration across southern and central Türkiye.

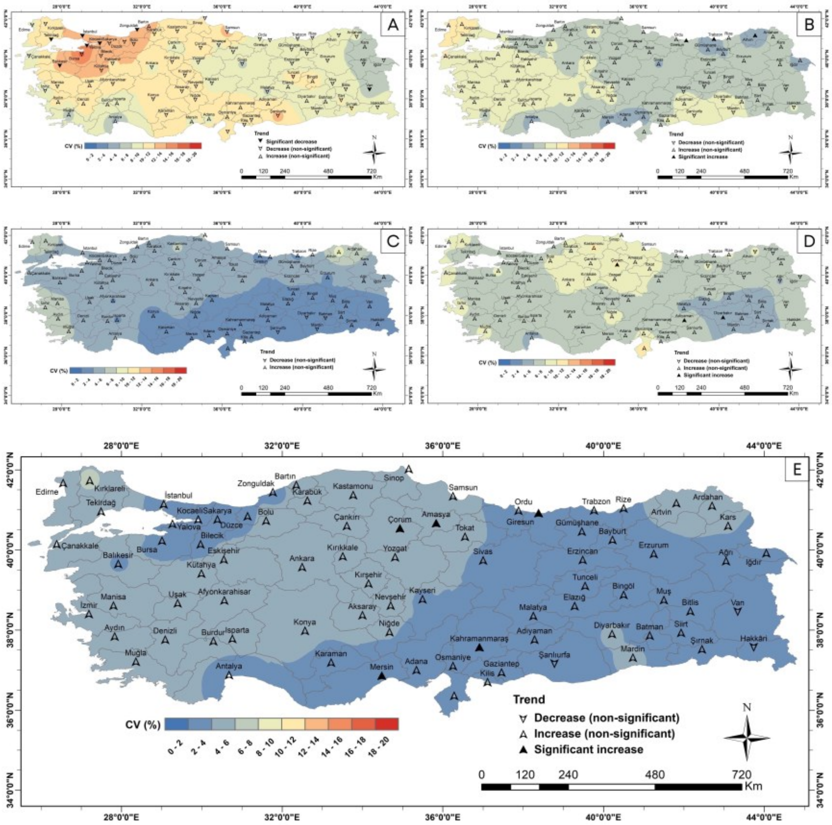

Figure 1. Spatial distribution of Spearman rank correlation and coefficient of variation of reference crop evapotranspiration during the reference period (1971-2000): (A) Winter; (B) Spring; (C) Summer; (D) Autumn; (E) Annual.

Under the near-future RCP4.5 scenario (2023-2052), the spatial and temporal distribution of ETo based on HADGEM outputs exhibited distinct regional contrasts across Türkiye (Figure 2). During winter, negative correlations remained concentrated over the Marmara Region, indicating a continuation of the declining tendencies identified in the reference period (Figure 2A). Conversely, the Southeastern Anatolia, Aegean, and Mediterranean regions displayed positive correlations, reflecting localized increases in evaporative demand. CV reached up to 18% in some southern areas, suggesting greater temporal instability. Spring patterns were largely dominated by positive correlations across the country, except for a weakly negative signal confined to Tekirdağ (Figure 2B). Significant monotonic increases were limited to Samsun, Gümüşhane, and Artvin, consistent with earlier findings that highlight temperature sensitivity in the Black Sea region (Guo et al. 2017). Although CV values were mostly homogeneous, inland provinces exhibited slightly higher variability, approaching 12%. In summer (Figure 2C), overall CV values remained low, confirming the climatic stability of season. Nonetheless, İzmir and Manisa showed moderate variability (8-10%), while Southeastern Anatolia exhibited strong positive correlations, implying enhanced evaporative conditions under warming influences. This agrees with previous regional analyses reporting notable ETo increases in southern Türkiye (Altındağ 2007; Nistor et al. 2019). Autumn revealed the most pronounced positive tendencies of all seasons, with negative correlations only appearing in the eastern Black Sea and Eastern Anatolia. Muğla recorded the highest CV values (up to 16%) indicating stronger intra-seasonal variability, possibly linked to transitional climatic effects between Mediterranean and continental influences (Figure 2D). At the annual scale, no significant negative correlations were detected. Positive trends prevailed throughout Türkiye, with the strongest associations found in the coastal Aegean, Southeastern, and Eastern Anatolia regions (Figure 2E).

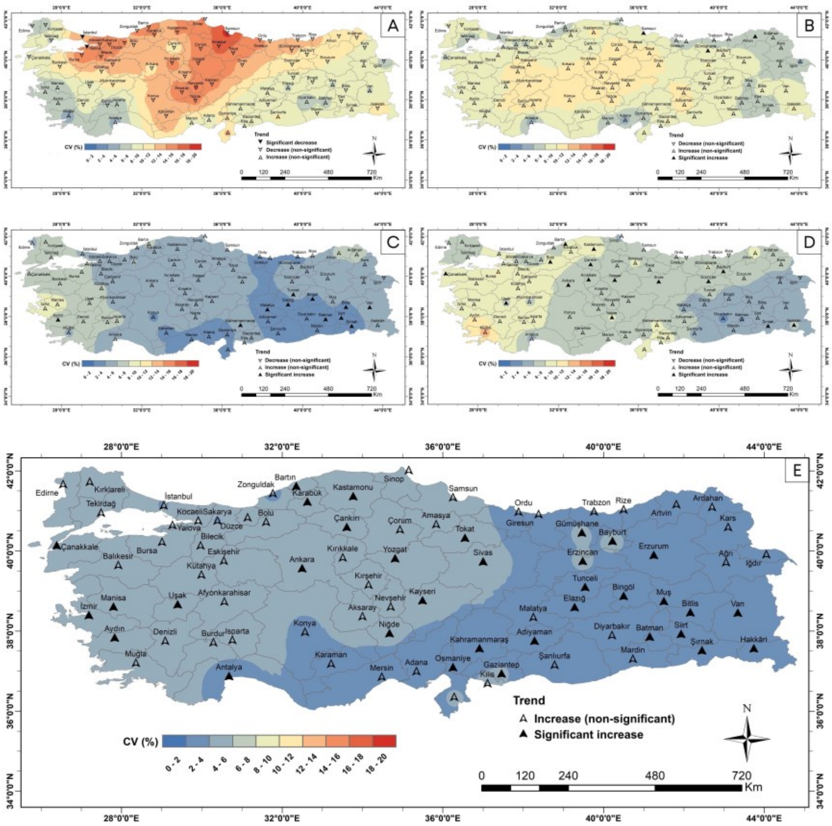

Figure 2. Spatial distribution of Spearman rank correlation and coefficient of variation of reference crop evapotranspiration under the near-future RCP4.5 scenario (2023-2052): (A) Winter; (B) Spring; (C) Summer; (D) Autumn; (E) Annual.

Under the near-future RCP8.5 scenario, the spatial and temporal variability of ETo exhibited marked contrasts across Türkiye (Figure 3). Negative correlations that dominated the Marmara Region in the reference period weakened considerably, persisting only around Kırklareli. Variability remained high in western Marmara, the central Black Sea, and parts of central Anatolia, where CV values reached 16%, while Çanakkale, Antalya, and Iğdır recorded the lowest dispersion (Figure 3A). Temperature-induced increases in ETo became more evident toward spring, when statistically significant upward tendencies covered almost the entire country. Except for the western Aegean and Marmara coasts, all regions (particularly Central, Eastern, and Southeastern Anatolia) showed strong monotonic increases, consistent with the findings of Guo et al. (2017) regarding the dominance of temperature in driving ETo variability (Figure 3B). The spatial pattern during summer revealed a relatively homogeneous distribution with low CV values overall. However, a clear belt of significant positive trends extended from Çanakkale to Kars, accompanied by additional clusters in Adana, Hatay, and Southeastern Anatolia. These results align with Nistor et al. (2019), who projected up to 20% ETo increases across southern Türkiye under similar radiative forcing (Figure 3C). Autumn displayed uniformly positive ETo trends across the country, with the strongest signals along the Black Sea coast. The CV values, mostly between 6% and 10%, indicated moderate intra-seasonal variability. Comparable autumnal behavior was previously described by Hui-Mean et al. (2018), who associated increased ETo in humid areas with prolonged dry intervals (Figure 3D). Annually, nearly all provinces except Mersin exhibited statistically significant upward correlations, while the overall CV distribution remained stable. This persistence of low interannual variability, despite intensifying evapotranspiration, underscores the robust influence of radiative forcing under the RCP8.5 scenario (Figure 3E).

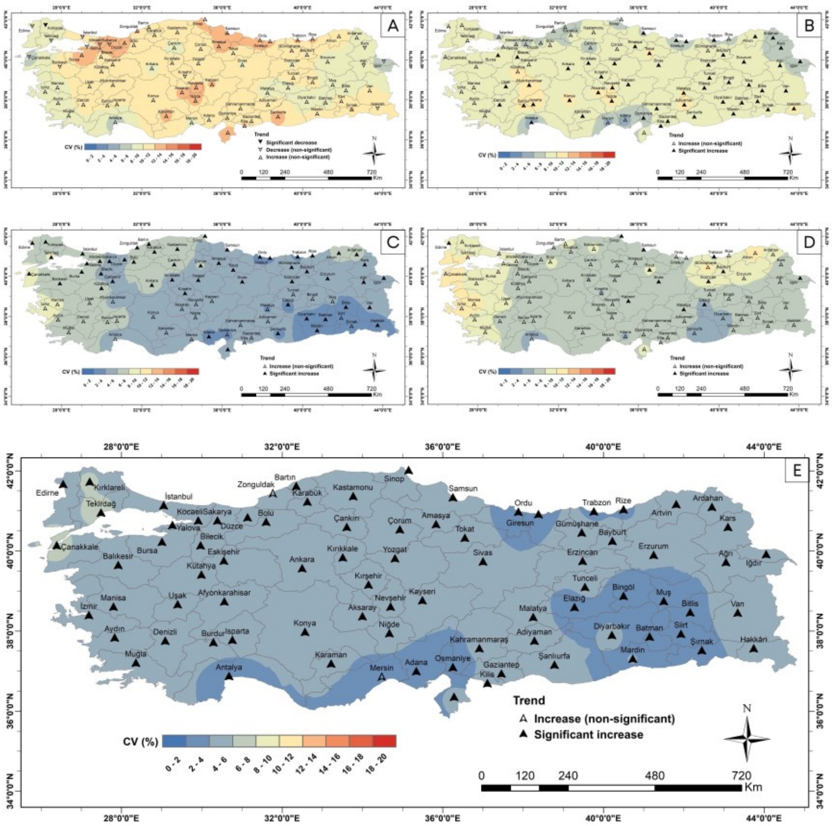

Figure 3. Spatial distribution of Spearman rank correlation and coefficient of variation of reference crop evapotranspiration under the near-future RCP8.5 scenario (2023-2052): (A) Winter; (B) Spring; (C) Summer; (D) Autumn; (E) Annual.

Under the far-future RCP4.5 scenario, ETo patterns across Türkiye reflected moderate but regionally distinct temporal variability. Statistically significant increases were concentrated in Mardin, Kahramanmaraş, and Şırnak, while the rest of the country exhibited mixed tendencies. The coefficient variation ranged from 4% to 16%, with higher variability observed in Central Anatolia and the Marmara-Black Sea transition zone, pointing to strong regional contrasts (Figure 4A). Seasonal behavior during spring showed no remarkable increase or decrease overall. Most provinces maintained neutral trends, though localized fluctuations were apparent in the Thrace region, where CV values reached 12%. These findings suggest that evapotranspiration in spring remains relatively stable under moderate radiative forcing, consistent with observations by Arabi and Candoğan (2022) of limited spring variability in northwestern Türkiye (Figure 4B). In summer, the correlation structure appeared spatially uniform with low CV values, reflecting stable temporal patterns. Although positive trends dominated, a few provinces such as Iğdır, Tunceli, and Elazığ displayed weak negative coefficients, none of which were statistically significant. Notably, the scattered yet prevailing positive correlations across Anatolia are consistent with projections by Guo et al. (2017), linking strong summer temperature rises to enhanced evapotranspiration (Figure 4C). Autumn revealed more defined spatial contrasts, with pronounced positive correlations in northern and central parts of Türkiye. Nearly all provinces in the northern Central Anatolia and eastern Black Sea regions exhibited statistically significant increases. The east-to-west rise in CV values indicates growing variability toward western Türkiye, echoing regional heterogeneity patterns highlighted by Hui-Mean et al. (2018) (Figure 4D). Annual results confirmed that Southeastern Anatolia remains the most sensitive zone, showing widespread significant increases in ETo. Only Iğdır registered a non-significant decrease, while most of the country maintained relatively low annual CV values. Such limited interannual variability implies stable yet upward-directed evapotranspiration trends, aligning with Nistor et al. (2019) who emphasized intensifying water demand and the need for adaptive irrigation strategies in southern Türkiye (Figure 4E).

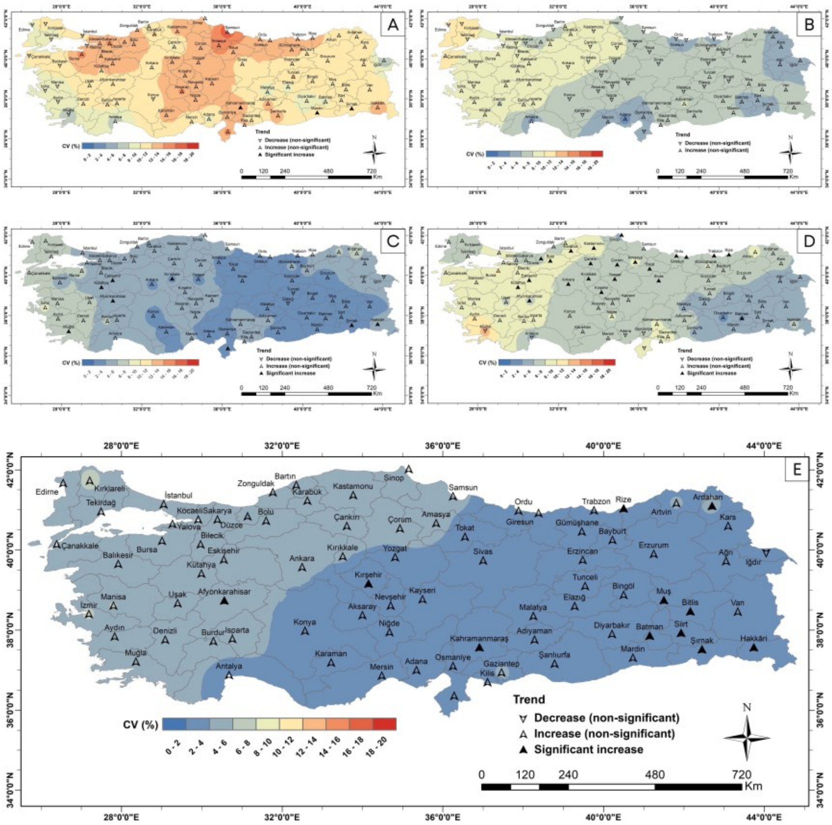

Figure 4. Spatial distribution of Spearman rank correlation and coefficient of variation of reference crop evapotranspiration under the far-future RCP4.5 scenario (2069-2098): (A) Winter; (B) Spring; (C) Summer; (D) Autumn; (E) Annual.

In the far-future RCP8.5 scenario of the HADGEM model, the winter map reveals generally upward tendencies across Türkiye except for parts of Eastern and Southeastern Anatolia (Figure 5A). Although most correlations were positive, no statistically significant trends were detected. Northern provinces exhibited higher CV values, locally exceeding 18%, indicating pronounced temporal variability in colder regions. Zeng et al. (2021) associated such non-significant winter trends with increased atmospheric humidity, while Tam et al. (2019) noted that precipitation variability under RCP8.5 may obscure clear ETo increases during this season. During spring (Figure 5B), ETo changes were not statistically significant. The CV values showed a more homogeneous distribution than in winter, ranging mostly between 2-12 %. Positive r_s values dominated the country except in Mersin, Hatay, and Osmaniye. This spatial coherence reflects the transitional behavior of meteorological drivers such as solar radiation and humidity noted by Chen and Robinson (2009). Summer (Figure 5C) exhibited the strongest and most widespread increases in ETo. The majority of stations showed statistically significant positive correlations, consistent with Guo et al. (2017), who reported that rising summer temperatures in the Northern Hemisphere are the main factor controlling ETo variations. The CV pattern displayed marked regional contrast, values reached 10% in Thrace but fell below 2% in Southeastern Anatolia, suggesting that interannual fluctuations are much smaller in the arid zones where temperature-driven processes dominate. Similar intensifications under RCP8.5 conditions were also reported by Liu et al. (2018) for Mediterranean-type climates. In autumn (Figure 5D), strong and significant positive trends were concentrated in western and southern Türkiye, particularly across northern Central Anatolia and the Mediterranean coast. Conversely, non-significant variations persisted along the Black Sea and southeastern provinces. Arabi and Candoğan (2022) likewise observed persistent increases across western regions during 1990-2020, whereas topographic controls highlighted by Chen and Robinson (2009) may explain the muted response over the coastal north. Annual averages (Figure 5E) revealed statistically significant upward tendencies across nearly all provinces except Siirt, Şırnak, and Şanlıurfa. The CV distribution remained largely homogeneous (2-6%), indicating temporal stability of ETo dynamics at the national scale. However, higher CV values in Thrace denote localized variability that may arise from land-use heterogeneity and maritime influences. The strong and consistent increases observed in Central and Southeastern Anatolia align with the findings of Altındağ (2007), Nistor et al. (2019), and Hui-Mean et al. (2018), who all emphasized that these regions face escalating evapotranspiration demand and growing irrigation water requirements under intensified climate-warming conditions.

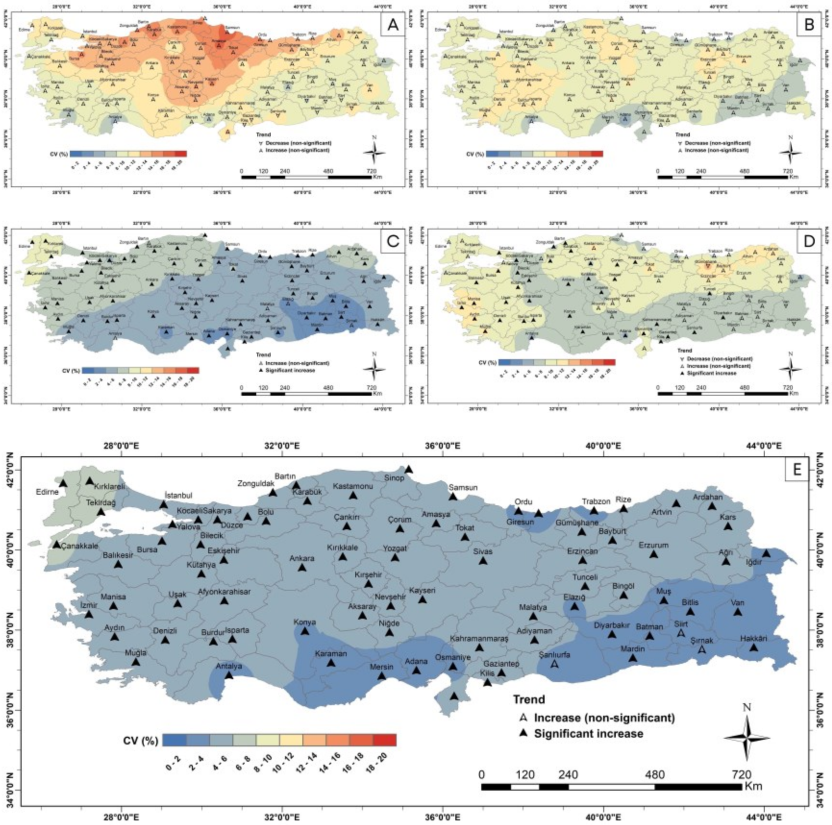

Figure 5. Spatial distribution of Spearman rank correlation and coefficient of variation of reference crop evapotranspiration under the far-future RCP8.5 scenario (2069-2098): (A) Winter; (B) Spring; (C) Summer; (D) Autumn; (E) Annual.

Analysis of the spatial and temporal variability derived from HADGEM projections indicates that Türkiye experiences a coherent yet regionally diverse response to climatic forcing. The magnitude and persistence of ETo trends intensify from the reference to the far-future periods, particularly under the RCP8.5 scenario, reflecting the growing influence of temperature and radiation on evaporative demand. Western and southern regions (especially the Aegean, Mediterranean, and Southeastern Anatolia) consistently exhibit strong and statistically significant upward tendencies, while northern and high-elevation areas remain comparatively stable. The accompanying CV maps highlight that the strength of monotonic trends does not necessarily correspond to temporal stability, as regions with high correlations often maintain substantial intra-period variability. Together, these spatial contrasts illustrate how climatic forcing may amplify evapotranspiration variability even in areas where long-term trends appear moderate, underscoring the uneven nature of hydroclimatic responses across Türkiye.

4. Conclusions

The results suggest that reference crop evapotranspiration may increase across much of Türkiye under the adopted HadGEM (RegCM4.3.4) RCP4.5 and RCP8.5 projection framework, with larger increases generally appearing in the far-future period and under RCP8.5. The magnitude and spatial structure of the projected response vary by season and region, with comparatively stronger increases in western, southern, and southeastern provinces. These findings should be interpreted as scenario-based provincial-scale estimates derived from a single adopted projection framework rather than as deterministic local forecasts. The study does not replace detailed station-scale validation, multi-model CMIP6 assessment, or topography-aware interpolation analyses, all of which remain important directions for future work. Even with these limitations, the results provide a useful first-order basis for discussing potential changes in evaporative demand and irrigation pressure under climate change in Türkiye.

Overall, the projected increases in ETo imply substantial challenges for sustainable agricultural water management and food security. Rising evaporative demand, especially under high-emission scenarios, may intensify irrigation requirements and exacerbate competition over limited freshwater resources. These results underscore the importance of adaptive management strategies that integrate efficient irrigation scheduling, crop pattern adjustment, and basin-scale water allocation planning. Continuous monitoring of climate-driven changes in ETo, supported by regional modeling and long-term observations, will be very important to ensuring agricultural resilience and sustainable resource use under a warming climate.

Author Contributions: Conceptualization, A.K.Y. and B.N.C.; methodology, A.K.Y. and B.N.C.; software, A.K.Y.; formal analysis, A.K.Y.; investigation, A.K.Y. and B.N.C.; writing—original draft preparation, A.K.Y.; writing—review and editing, B.N.C.; visualization, A.K.Y.; supervision, B.N.C. All authors have read and agreed to the published version of the manuscript.

Funding: This research received no external funding

Acknowledgments: This study contains partial findings of the PhD dissertation of Ali Kaan Yetik. The authors are gratefully acknowledged to the Turkish State Meteorological Service for sharing meteorological data used for this study.

Conflicts of Interest: The authors declare no conflict of interest.

References

Akçakaya, A., Sümer, U. M., Demircan, M., Demir, Ö., Atay, H., Eskioğlu, O., Gürkan, H., & Çukurçayır, F. (2015). *Yeni Senaryolarla Türkiye İklim Projeksiyonları ve İklim Değişikliği - TR2015-CC*. Meteoroloji Genel Müdürlüğü Yayını, Ankara, Turkey. p.149.

Allen, R. G., Pereira, L. S., Raes, D., & Smith, M. (1998). Crop Evapotranspiration - Guidelines for Computing Crop Water Requirements (FAO Irrigation and Drainage Paper 56). FAO, Rome, Italy.

Altındağ, M. (2007). GAP alanında farklı yöntemlere göre hesaplanan referans bitki su tüketimi değerlerinin gidiş analizi. MSc Thesis, Harran University, Institute of Science (Unpublished), Turkey.

Arabi, C., & Candoğan, B. N. (2022). Marmara Bölgesinde referans bitki su tüketiminin alansal ve zamansal değişimi. *Uluslararası Tarım ve Yaban Hayatı Bilimleri Dergisi* 8(2): 268-281. https://doi.org/10.24180/ijaws.1080376.

Arslan, O. (2017). Niğde ili'ndeki potansiyel evapotranspirasyon tahminlerinin trend analizi. *Niğde Ömer Halisdemir Üniversitesi Mühendislik Bilimleri Dergisi* 6(2): 602-608.

Ayas, S. (2019). Water-yield relationships in deficit irrigated onion. *Turkish Journal of Agriculture-Food Science and Technology* 7(9): 1310-1320. https://doi.org/10.24925/turjaf.v7i9.1310-1320.2533

Bora, E., Tekeli, M., & Etöz, M. (2015). Menemen Ovasında referans bitki su ihtiyacı ve ölçülen solar radyasyonun zamansal değişimi. *Anadolu Ege Tarımsal Araştırma Enstitüsü Dergisi* 25(2): 65-76.

Calzadilla, A., Rehdanz, K., & Tol, R. S. (2010). The economic impact of more sustainable water use in agriculture: A computable general equilibrium analysis. *Journal of Hydrology* 384(3-4): 292-305. https://doi.org/10.1016/j.jhydrol.2009.12.012.

Chen, F., & Robinson, P. J. (2009). Estimating reference crop evapotranspiration with ETgages. *Journal of Irrigation and Drainage Engineering* 135(3): 335-342. https://doi.org/10.1061/(ASCE)IR.1943-4774.0000005.

Danandeh Mehr, A., Sorman, A. U., Kahya, E., & Hesami Afshar, M. (2020). Climate change impacts on meteorological drought using SPI and SPEI: Case study of Ankara, Turkey. *Hydrological Sciences Journal* 65(2): 254-268. https://doi.org/10.1080/02626667.2019.1691218.

Demircan, M., Gürkan, H., Eskioğlu, O., Arabacı, H., & Coşkun, M. (2017). Climate change projections for Turkey: three models and two scenarios. Turkish Journal of Water Science and Management 1(1): 22-43. https://doi.org/10.31807/tjwsm.297183.

Deveci, H., & Konukcu, F. (2024). Modeling the effect of climate change on evapotranspiration in the Thrace Region. *Atmosphere* 15(10): 1188. https://doi.org/10.3390/atmos15101188.

Di Nunno, F., & Granata, F. (2023). Future trends of reference evapotranspiration in Sicily based on CORDEX data and machine learning algorithms. *Agricultural Water Management* 280: 108232. https://doi.org/10.1016/j.agwat.2023.108232.

Droogers, P., & Allen, R. G. (2002). Estimating reference evapotranspiration under inaccurate data conditions. *Irrigation and Drainage Systems* 16: 33-45. https://doi.org/10.1023/A:1015508322413.

Easterling, D. R., Meehl, G. A., Parmesan, C., Changnon, S. A., Karl, T. R., & Mearns, L. O. (2000). Climate extremes: observations, modeling, and impacts. *Science* 289(5487): 2068-2074. https://doi.org/10.1126/science.289.5487.2068.

Fan, J., Wu, L., Zhang, F., Xiang, Y., & Zheng, J. (2016). Climate change effects on reference crop evapotranspiration across different climatic zones of China during 1956-2015. *Journal of Hydrology* 542: 923-937. https://doi.org/10.1016/j.jhydrol.2016.09.060.

Gomez-Zavaglia, A., Mejuto, J. C., & Simal-Gandara, J. (2020). Mitigation of emerging implications of climate change on food production systems. *Food Research International* 134: 109256. https://doi.org/10.1016/j.foodres.2020.109256.

Guo, D., Westra, S., & Maier, H. R. (2017). Sensitivity of potential evapotranspiration to changes in climate variables for different Australian climatic zones. *Hydrology and Earth System Sciences* 21(4): 2107-2126. https://doi.org/10.5194/hess-21-2107-2017.

He, D., Liu, Y., Pan, Z., An, P., Wang, L., Dong, Z., & Zhao, P. (2013). Climate change and its effect on reference crop evapotranspiration in central and western Inner Mongolia during 1961-2009. *Frontiers of Earth Science* 7: 417-428. https://doi.org/10.1007/s11707-013-0381-z.

Helsel, D. R., & Hirsch, R. M. (1993). *Statistical Methods in Water Resources*. Elsevier.

Hui-Mean, F., Yusop, Z., & Yusof, F. (2018). Drought analysis and water resource availability using standardized precipitation evapotranspiration index. *Atmospheric Research* 201: 102-115. https://doi.org/10.1016/j.atmosres.2017.10.014.

Jun, W., Xinhua, W., Meihua, G., & Xuyan, X. U. (2012). Impact of climate change on reference crop evapotranspiration in Chuxiong City, Yunnan Province. *Procedia Earth and Planetary Science* 5: 113-119. https://doi.org/10.1016/j.proeps.2012.01.019.

Karaer, M., Gültaş, H. T., & Kuşçu, H. (2023). The effects of plastic mulched drip irrigation on yield, fruit quality and water productivity of table tomatoes. *Gesunde Pflanzen* 75(5): 1591-1599. https://doi.org/10.1007/s10343-023-00848-x

Kingra, P. K., Setia, R., Aatralarasi, S., Kukal, S. S., & Singh, S. P. (2024). Spatio-temporal variability in evapotranspiration and moisture availability for crops under future climate change scenarios in north-west India. *Arabian Journal of Geosciences* 17(4): 126. https://doi.org/10.1007/s12517-024-11921-8.

Kum, G. (2022). Yarıkurak sahalarda referans evapotranspirasyonun (ETo) alansal dağılımı ve zamansal değişimi: Şanlıurfa örneği. *Türk Coğrafya Dergisi* 80: 87-96. https://doi.org/10.17211/tcd.1116059.

Landsea, C. W., & Gray, W. M. (1992). The strong association between western Sahelian monsoon rainfall and intense Atlantic hurricanes. *Journal of Climate* 5(5): 435-453. https://doi.org/10.1175/1520-0442(1992)005<0435:TSABWS>2.0.CO;2.

Lebel, T., Bastin, G., Obled, C., & Creutin, J. D. (1987). On the accuracy of areal rainfall estimation: a case study. *Water Resources Research* 23(11): 2123-2134. https://doi.org/10.1029/WR023i011p02123.

Leng, G., Tang, Q., & Rayburg, S. (2015). Climate change impacts on meteorological, agricultural and hydrological droughts in China. *Global and Planetary Change* 126: 23-34. https://doi.org/10.1016/j.gloplacha.2015.01.003.

Li, Z., Xu, X., Yu, B., Xu, C., Liu, M., & Wang, K. (2016). Quantifying the impacts of climate and human activities on water and sediment discharge in a karst region of southwest China. *Journal of Hydrology* 542: 836-849. https://doi.org/10.1016/j.jhydrol.2016.09.049.

Liu, Q., Yan, C., Ju, H., & Garré, S. (2018). Impact of climate change on potential evapotranspiration under a historical and future climate scenario in the Huang-Huai-Hai Plain, China. *Theoretical and Applied Climatology* 132: 387-401. https://doi.org/10.1007/s00704-017-2060-6.

Liu, Z., Lu, J., Huang, J., Chen, X., & Zhang, L. (2021). Projection of reference crop evapotranspiration under future climate change in Poyang Lake watershed, China. *Journal of Hydrologic Engineering* 26(1): 05020042. https://doi.org/10.1061/(ASCE)HE.1943-5584.0002020.

Lu, G. Y., & Wong, D. W. (2008). An adaptive inverse-distance weighting spatial interpolation technique. Computers & geosciences, 34(9): 1044-1055. https://doi.org/10.1016/j.cageo.2007.07.010

McMichael, A. J., & Lindgren, E. (2011). Climate change: present and future risks to health, and necessary responses. *Journal of Internal Medicine* 270(5): 401-413. https://doi.org/10.1111/j.1365-2796.2011.02415.x.

Meehl, G. A., Zwiers, F., Evans, J., Knutson, T., Mearns, L., & Whetton, P. (2000). Trends in extreme weather and climate events: issues related to modeling extremes in projections of future climate change. *Bulletin of the American Meteorological Society* 81(3): 427-436. https://doi.org/10.1175/1520-0477(2000)081<0427:TIEWAC>2.3.CO;2.

Mojid, M. A., Rannu, R. P., & Karim, N. N. (2015). Climate change impacts on reference crop evapotranspiration in north-west hydrological region of Bangladesh. *International Journal of Climatology* 35(13). https://doi.org/10.1002/joc.4260.

Montgomery, D. C., & Runger, G. C. (2010). *Applied Statistics and Probability for Engineers*. John Wiley & Sons.

Myers, S. S., & Patz, J. A. (2009). Emerging threats to human health from global environmental change. *Annual Review of Environment and Resources* 34: 223-252. https://doi.org/10.1146/annurev.environ.033108.102650.

Nistor, M. M., Mîndrescu, M., Petrea, D., Nicula, A. S., Rai, P. K., Benzaghta, M. A., & Porumb-Ghiurco, C. G. (2019). Climate change impact on crop evapotranspiration in Turkey during the 21st century. *Meteorological Applications* 26(3): 442-453. https://doi.org/10.1002/met.1774.

Raes, D., & Muñoz, G. (2009). *The ETo Calculator: Reference Manual Version 3.1*. FAO, Rome. http://www.fao.org/land-water/databases-and-software/eto-calculator/en/ (access date: 05.07.2025).

Reid, P. C., Fischer, A. C., Lewis-Brown, E., Meredith, M. P., Sparrow, M., Andersson, A. J., & Washington, R. (2009). Impacts of the oceans on climate change. *Advances in Marine Biology* 56: 1-150. https://doi.org/10.1016/S0065-2881(09)56001-4.

Shamir, E., Mendoza Fierro, L., Mohsenzadeh Karimi, S., Pelak, N., Tarouilly, E., Chang, H. I., & Castro, C. L. (2024). Climate change projections of potential evapotranspiration for the North American monsoon region. *Hydrology* 11(6): 83. https://doi.org/10.3390/hydrology11060083.

Singh, V. P., & Chowdhury, P. K. (1986). Comparing some methods of estimating mean areal rainfall 1. *JAWRA Journal of the American Water Resources Association* 22(2): 275-282. https://doi.org/10.1111/j.1752-1688.1986.tb01884.x.

Tam, B. Y., Szeto, K., Bonsal, B., Flato, G., Cannon, A. J., & Rong, R. (2019). CMIP5 drought projections in Canada based on the standardized precipitation evapotranspiration index. *Canadian Water Resources Journal* 44(1): 90-107. https://doi.org/10.1080/07011784.2018.1537812.

Thomas, A. (2000). Spatial and temporal characteristics of potential evapotranspiration trends over China. *International Journal of Climatology* 20(4): 381-396. https://doi.org/10.1002/(SICI)1097-0088(20000330)20:4<381::AID-JOC477>3.0.CO;2-K.

Ünlükara, A., Yürekli, K., Aküzüm, T., Örs, İ., & Safi, S. (2011). Konya ve Karaman illerinde bitki su tüketimi (ETo) değişiminin analizi. *Tarım Bilimleri Araştırma Dergisi* 1: 1-5.

Walter, I. A., Allen, R. G., Elliott, R., Jensen, M. E., Itenfisu, D., Mecham, B., & Martin, D. (2000). ASCE's standardized reference evapotranspiration equation. *Watershed Management and Operations Management* 2000: 1-11. https://doi.org/10.1061/9780784408056.fm.

Woyessa, Y. E. (2024). Sustainable management of water resources in a semi-arid river basin under climate change: a case study in South Africa. In *BRICS Countries: Sustainable Water Resource Management and Pollution Control: Challenges and Opportunities*. Springer, Singapore, pp. 183-209. https://doi.org/10.1007/978-981-99-9581-3_8.

Yetik, A. K., Arslan, B., & Şen, B. (2024). Trends and variability in precipitation across Turkey: a multimethod statistical analysis. Theoretical and Applied Climatology 155: 473-488. https://doi.org/10.1007/s00704-023-04645-4.

Zar, J. H. (2005). Spearman rank correlation. In *Encyclopedia of Biostatistics*, Vol. 7. https://doi.org/10.1002/0470011815.b2a15150.

Zeng, P., Sun, F., Liu, Y., Feng, H., Zhang, R., & Che, Y. (2021). Changes of potential evapotranspiration and its sensitivity across China under future climate scenarios. *Atmospheric Research* 261: 105763. https://doi.org/10.1016/j.atmosres.2021.105763.